

Dynamics of Glasses and Glass-Forming Liquids Studied by Inelastic X-ray Scattering

Francesco Sette,* Michael H. Krisch, Claudio Masciovecchio, Giancarlo Ruocco, Giulio Monaco

The development of inelastic x-ray scattering with millielectron volt energy resolution at the European Synchrotron Radiation Facility in Grenoble, France, provides a method for studying high-frequency collective dynamics in disordered systems. This has led to the observation of propagating acoustic phonon-like excitations in glasses and glass-forming liquids down to wavelengths comparable to the interparticle distance. Using the inelastic x-ray scattering results on glycerol as a representative example, it is shown that the microscopic dynamic properties are related to the excess of vibrational states in glasses and to the consequences at the microscopic level of the liquid-glass transition. Moreover, they allow derivation of the infinite frequency sound velocity, a quantity related to the structural relaxation times and to the change of ergodicity at the liquid-glass transition.

One of the challenges of condensed matter physics is the “microscopic” understanding of “macroscopic” phenomena, ranging from those common to all materials, such as thermal expansion, thermal conductivity, specific heat, and dielectric properties, to more specific ones, such as magnetism, superconductivity, and superfluidity. In crystalline systems, the crystal translational invariance reduces the investigated problem to that of a relatively small number of atoms, constituting the crystal unit cell. Thanks to this simplification, advanced solid-state “classical” and “quantum” theories have become computationally amenable in spite of their conceptual complexity. For example, atomic motions in crystals can be described in terms of collective oscillations around equilibrium positions, and these microscopic vibrational dynamics can be linked to a large class of macroscopic phenomena.

Qualitative differences occur as soon as the microscopic crystalline order is abandoned (1, 2), as in the liquid and glass phases. In contrast to the crystalline case, the disordered system is characterized by two different length-scales: in addition to the interparticle separation, a , one must also consider the correlation length characterizing the topological disorder, ξ . Moreover, the understanding of the atomic dynamics is complicated not only by the difficulties associated with the absence of translational invariance, but also by the presence of other degrees of freedom, such

as diffusion and relaxation in fluids (3) and hopping and tunneling processes in glasses (4). The presence of these processes in disordered systems naturally introduces a time scale, τ , usually strongly dependent on the specific thermodynamic state. This time scale affects the collective dynamical properties differently, depending on its value with respect to the time scale t_D characterizing the “vibrational” dynamics of the particles around their quasi-equilibrium position. This is of the order of $t_D \approx 1/\omega_D$, where $\omega_D = v(6\pi^2\rho)^{1/3}$ is the Debye frequency, whose value is comparable to that of a corresponding crystal with similar number density, ρ , and sound velocity, v . The rich phenomenology observed in the dynamics of disordered systems is often the consequence of the interplay between these different structural (a , ξ) and dynamic (τ , t_D) scales.

The collective dynamics in the absence of translational invariance can easily be treated theoretically in two limiting cases—namely, excitations with characteristic space and time scales which are either very long or very short compared to the disorder scale ξ and to the relaxation time τ , respectively. They are, respectively, the hydrodynamic limit, where the system is seen as a continuum, and the single-particle limit, where the particle behavior is described as a free particle between successive collisions. In contrast, an exhaustive theoretical understanding is still not available in the intermediate, mesoscopic region, defined by a length scale comparable to the correlation length of the topological disorder and by a time scale comparable to t_D (3).

On the experimental side, in crystals, the mesoscopic space-time domain—corresponding to a momentum-energy region of

0.01 to 10 nm⁻¹ and 0.1 to 20 meV—is traditionally studied by inelastic neutron scattering (INS) (5). In disordered systems, the neutron technique has been successfully used to investigate the dynamics at momentum transfer typically larger than 10 nm⁻¹ (6, 7). In the mesoscopic scale, because of the typical kinematic conditions of the scattering process, neutrons cannot easily probe the acoustic branch as soon as the speed of sound, v , of the considered disordered material has a value larger than $v \approx 1500$ m/s. Considering that the typical values of v in glasses and liquids are either comparable or considerably larger than 1500 m/s, it can be explained why, in disordered systems, a comprehensive experimental picture of the high-frequency collective dynamics is still missing.

The outlined experimental and theoretical scenario has left open several relevant questions on the mesoscopic dynamics of disordered materials. Among them are the following: (i) Are there collective excitations in liquids and glasses with wavelengths approaching ξ and a ? And, if so, to what extent do their eigenvectors deviate from the plane waves found in crystals? Are these deviations responsible for the anomalous thermal conductivity found in glasses at low temperatures? Similarly, how do they relate to the sound excitations observed in the long wavelength limit? (ii) With respect to the Debye behavior of the corresponding crystal, what is the origin of the excess specific heat at low temperature and the excess density of vibrational states found in glasses? (iii) What is the microscopic description of hopping and tunneling phenomena in glasses, and of relaxation processes in liquids? (iv) Are short-wavelength excitations still affected by relaxation processes as observed for those at long wavelengths? This last point relates to the issue of how the high-frequency dynamics may be affected by the liquid-glass transition in glass-forming systems and whether any critical behavior is present in these dynamics.

Inelastic X-ray Scattering with Millielectron Volt Energy Resolution

Inelastic x-ray scattering (IXS) with 10 to 20 keV incident energy (8) is, in principle, a complementary method to INS for

F. Sette, M. H. Krisch, and C. Masciovecchio are at the European Synchrotron Radiation Facility (ESRF), Boite Postale 220 F-38043, Grenoble, Cedex France. G. Ruocco and G. Monaco are at the Università di L'Aquila and Istituto Nazionale di Fisica della Materia, I-67100, L'Aquila, Italy.

*To whom correspondence should be addressed. E-mail: sette@esrf.fr

studying acoustic excitations at small momentum transfer. The interest in using x-rays come from the fact that, whenever the probe particle incident energy is much higher than the exchanged energy, kinematic limitations are no longer relevant. Therefore, the desired phase space can be easily accessed. This is the case using x-rays, if one can achieve sufficient energy resolution and incident beam intensity.

The IXS technique is a very recent development that was made possible by the high x-ray spectral flux density available from an undulator at the new third-generation synchrotron radiation sources (9) and by new ideas in perfect crystals optics that allowed an energy resolution in the millielectron volt range, corresponding to a resolving power of $\sim 10^7$ (10–12). This has permitted the construction of a new instrument, which has been in operation since 1995 at the European Synchrotron Radiation Facility in Grenoble. Its main success lies in the capability to access the mesoscopic (Q – E) region, providing the opportunity to measure the dynamic structure factor $S(Q, E)$ at momentum transfers, Q , in the 0.5 to 30 nm^{-1} range with basically unlimited energy transfers, E . The quantity $S(Q, E)$ is the space and time Fourier transform of the particle density correlation function, and therefore, contains important information on the collective dynamics. An energy resolution of $1.5 \pm 0.2 \text{ meV}$ at full-width-half-maximum has been obtained in the energy analysis of $\sim 20\text{-keV}$ x-rays. An incident wavelength $\lambda_i = 0.05701 \text{ nm}$ (photon energy $E_i = 21,748 \text{ keV}$) is used, corresponding to the effective lattice parameter of the Si(11 \sim 11 \sim 11) Bragg reflection in a silicon perfect crystal. Other typical instrumental parameters are a Q resolution of $\pm 0.2 \text{ nm}^{-1}$, a beamsize on the sample of 0.1 mm by 0.3 mm , and a photon flux of $\sim 2 \times 10^8$ photons/s.

The intensity scattered in a solid angle $\Delta\Omega$ around \vec{Q} and in the energy interval ΔE around E [measured in an IXS experiment dominated by the pure charge (Thomson) scattering term] is proportional to the following double differential cross section (13)

$$\frac{\partial^2 \sigma}{\partial \Omega \partial E} = r_o^2 \frac{E_i}{E_f} |f(Q)|^2 S(Q, E) \quad (1)$$

where $r_o = 2.82 \times 10^{-15} \text{ m}$ is the classical electronic radius and $f(Q)$ is the electronic form factor of the scattering particles, which reduces (in the small Q limit) to the particle's number of electrons, Z . The energies E_i and E_f are those of the incident and scattered photons, respec-

tively. The proportionality to $S(Q, E)$ indicates that the spectrum of the density fluctuations of the system is directly obtained by measuring the scattered x-rays as a function of E and Q . This information is equivalent to that obtained from coherent INS measurements. Consequently, as long as an energy resolution in the millielectron volt range is sufficient, the IXS technique is a complementary tool to INS methods. Its main difference to INS is that it allows unlimited energy transfers in the accessible Q transfer range, namely in the ~ 1 to 100 nm^{-1} region. The main domain of application of the IXS tech-

nique has been, so far, the study of the high-frequency dynamics of liquids and glasses with the aim of contributing to the understanding of issues such as those outlined above. Other important areas of applications where this complementarity has not yet been exploited are the study of the dynamics of materials, even crystals, in cases where INS cannot provide useful information because of insufficient sample material, incoherent scattering from the sample isotope composition and nuclear spin orientation, or data reduction problems due to multiple scattering processes.

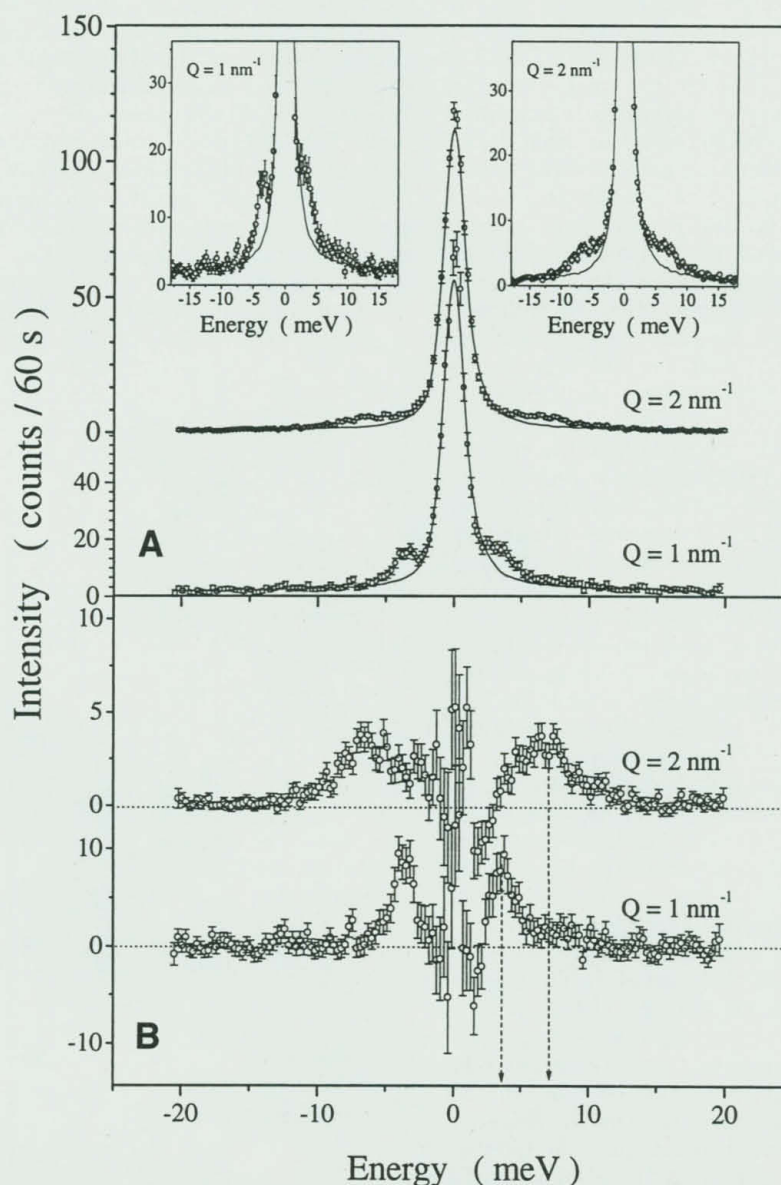


Fig. 1. (A) IXS spectra (\circ) of vitreous silica taken at $T = 1075 \text{ K}$ at $Q = 1$ and 2 nm^{-1} , with a total integration time of 415 and 800 s, respectively. The full curves are the measured resolution functions, which have been aligned and scaled to the central peak. The two insets are shown to emphasize the inelastic signal on the two sides of the central peak. **(B)** Difference spectra, obtained from the subtraction of the scaled resolution function from the spectra reported in (A). The inelastic peak energy positions, indicated by the dotted lines with arrows, scale approximately with the Q transfer.

Inelastic X-ray Scattering from Glasses and Glass-Forming Liquids

Extended IXS studies have been performed so far in several glasses and liquids, as well as across the liquid-glass transition. The investigated systems range from strong network-forming glasses to fragile and polymeric ones, also including different glass-forming liquids. These are SiO_2 , $\text{LiCl}\cdot 6\text{H}_2\text{O}$, CKN , *o*-terphenyl, *poly*-butadiene, *n*-butylbenzene, and *poly*-methyl-methacrylate (14, 15). In all these systems, it has been possible to observe a clear inelastic signal which also shows a marked Q dependence. To illustrate the main features of this IXS signal, we report two spectra (Fig. 1) taken at $Q = 1$ and 2 nm^{-1} in vitreous SiO_2 at $T = 1075 \text{ K}$. In Fig. 1A, the total spectra are compared to the experimentally determined resolution function, which has been aligned with the dominant peak centered at zero energy transfer (elastic peak). This peak is due to the frozen density fluctuations existing in glasses at all Q values, and therefore, it is very narrow; its broadening is due to the finite energy resolution. At both sides of this peak, the presence of an inelastic feature is observed, emphasized in the insets. The difference spectra, obtained by subtracting the central peak (represented by the resolution function) from the data, are reported in Fig. 1B in order to highlight the inelastic signal and its Q dependence. It can be observed that the average energy position and width of the signal increases with increasing Q . In particular, the two arrows show that the energy position doubles with the doubling of the Q transfer. This behavior is the one expected for propagating sound excitations: a similar result has been found in all liquids and glasses investigated so far by IXS. This general finding, implying that the sound mode extends into the investigated mesoscopic region, is shown in Fig. 1 as the result of a qualitative procedure which has the advantage of being model independent. A thorough analysis will be developed in the following discussion.

Inelastic x-ray scattering data collected from glycerol (16), one of the prototypical glass-forming liquids, are chosen here to illustrate some of the general features of the high-frequency dynamics of glasses and liquids, which have been observed in IXS studies. According to Angell's definition (17), glycerol is an example of an intermediate, hydrogen-bonded glass-former, and it has also been extensively investigated by Brillouin light scattering (BLS) and INS methods (18–20). The IXS spectrum of glycerol taken in the glass phase at $T = 175 \text{ K}$ and at $Q = 2 \text{ nm}^{-1}$ (Fig. 2) has three components, and, similarly to the SiO_2 data

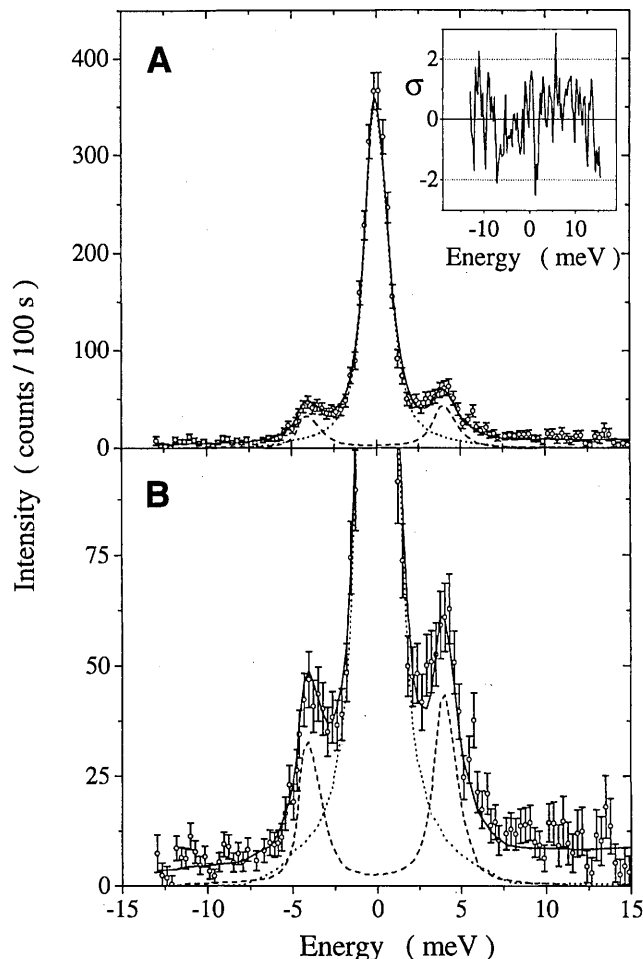
of Fig. 1, it looks very much like the typical Brillouin triplet observed in BLS measurements (21). Again, the existence of two inelastic features demonstrates the existence of well-defined excitations up to the energy and momentum considered here. To extract the spectroscopic parameters, such as the energy position $[\Omega(Q)]$ and the width $[\Gamma(Q)]$ of the inelastic features, as well as the intensities of the central and side peaks, we used a fitting procedure based on the convolution of the experimentally determined resolution function with a model function (Fig. 2). We used a Lorentzian to represent the central line, because this allows us, going from the glass to the liquid, to monitor the appearance of quasi-elastic scattering, present in the liquid as a consequence of relaxational and diffusional processes. We used a damped harmonic oscillator (DHO) (22) to represent the inelastic peaks. This DHO model can be derived theoretically as the high-frequency limit of the $S(Q, \omega)$ lineshape obtained within the generalized hydrodynamic theory (23). The typical resulting fit is exemplified by the solid line on the data and by the individual contributions, all shown separately in Fig. 2.

We report three sets of data (Fig. 3)

obtained at different Q values in the glass, $T = 175 \text{ K}$ ($T_g = 185 \text{ K}$); in the liquid, $T = 292 \text{ K}$; and as a function of T at the fixed Q value of 2 nm^{-1} . The inelastic features in the glass spectra (Fig. 3A) show a marked Q dependence increasing in energy and becoming progressively broader with increasing Q . A similar behavior is also found in the liquid (Fig. 3B). This Q dependence indicates the persistence of the propagating character of the collective dynamics up to these high frequencies. Besides the qualitative similarities between the liquid and the glass data, the temperature dependence of the features at fixed Q (Fig. 2C) shows that there is an evolution of the spectral shape in the glass transition region:

The spectra were analyzed as outlined above. The Q dependence of the excitation energies, $\Omega(Q)$, is almost linear in the whole examined Q range in both liquid and glass (Fig. 4A). This implies that these excitations have an acoustic nature, and their sound velocity is given by $v(Q) = \Omega(Q)/Q$. This confirms the qualitative analysis of Fig. 1, and, in the glass, the value of $v(Q)$ is consistent with that of low-frequency determinations. A different Q dependence is

Fig. 2. (A) IXS spectrum of glycerol at 175 K and $Q = 2 \text{ nm}^{-1}$, taken with energy and momentum resolutions $\Delta E = 1.5 \text{ meV}$ and $\Delta Q = 0.4 \text{ nm}^{-1}$ full-width-half-maximum, respectively. The data (\circ), shown with the error bars, are superimposed to the fit (solid line) as explained in the text. The dotted and dashed lines represent the quasi-elastic and inelastic contributions, respectively, to the total fits. (B) Enlargement of (A). The inset in (A) shows the residuals between the data and the fit in standard deviation units, σ .



found for the broadening, $\Gamma(Q)$, which is well represented by a Q^2 law (Fig. 4B). This law has also been observed in the other glasses investigated by IXS (14), and recently, it has been demonstrated to hold in a Q range wider than two decades (0.04 to 6 nm^{-1}) (15, 24). The equivalence of the $\Gamma(Q)$ values in the liquid and in the glass (Fig. 4B), in spite of the very different temperatures, indicates that the origin of the broadening is structural rather than dynamical, in the sense that it cannot be associated to a relaxation process. A similar temperature independence of $\Gamma(Q)$ has been observed in an extended temperature study of vitreous SiO_2 (15) and *o*-terphenyl (24). A possible explanation of this behavior can be found, considering that even in a "harmonic" and relaxation-free disordered system, a density fluctuation with wavevector Q is not an "eigenstate" as a consequence of the lack of translational invariance. This leads to a decay of the density fluctuation energy toward other degrees of freedom, and therefore, to a broadening of the inelastic peak. The observed Q^2 law only accidentally corresponds to the hydrodynamic prediction; it does not have, to our knowledge, any theoretical explanation.

A consequence of the different Q dependence of $\Omega(Q)$ and $\Gamma(Q)$ is the possibility of defining a Q value, Q_m , where $\Omega(Q_m) = \Gamma(Q_m)$. At Q_m , the two relations start to deviate from their simple Q laws, and for even higher Q values, it was not possible to

identify in the spectra a specific excitation feature. We propose to associate this Q_m value with the length scale characterizing the topological disorder, marking the transition from a collective acoustic-like behavior toward more localized dynamics. Studies of other glasses show that the Q_m value increases with fragility. This behavior can be summarized by a dimensionless parameter defined as Q_m/Q_M , where Q_M is the Q value of the first sharp diffraction peak in the static structure factor. We also find that Q_m/Q_M increases with fragility, going from ~ 0.15 in SiO_2 to ~ 0.3 in glycerol, and to ~ 0.5 in *o*-terphenyl (14, 15).

In Fig. 4A, E_{BP} corresponds to the energy of the "boson peak" in glycerol. The boson peak is a general feature of all glasses found in the incoherent INS and Raman spectra at energies in the 2- to 10-meV region (6, 25, 26). Specifically, it is a broad peak in the quantity $g(E)/E^2$, where $g(E)$ is the density of states. It, therefore, marks an excess of states (EoS), with respect to the Debye theory, that would predict $g(E)/E^2 = \text{const}$. This EoS is also responsible for the presence of a bump in the temperature dependence of C/T^3 (27, 28), where C is the specific heat. The nature of the EoS in glasses is still a subject of speculation, and at present, there are two different prevailing hypotheses (29). In the first, the EoS is explained by the localization of the vibrational modes induced by the static disorder in the glass. In the second, the EoS reflects

the density of states of collective propagating modes, which persist at high frequency. In the first view, the boson peak energy corresponds to the energy of the high Q excitations, whereas, in the second one the excitations are expected to propagate at energies above E_{BP} . The dispersion relations of the inelastic excitations, such as those reported in Fig. 4A, show that the propagation is systematically observed up to energies more than twice the boson peak energy. This finding, and the absence of any observable Q -independent feature at E_{BP} , strongly contradicts the first point of view. Consequently, and in agreement with recent molecular dynamics (MD) simulations (30), the IXS data support the second point of view. As suggested from those MD calculations, eigenvectors, which are consistent with the observed dispersion relations of $\Omega(Q)$ and $\Gamma(Q)$, can be expressed as the sum of a Q -dependent plane-wave component and an extended random uncorrelated component (30). The first component accounts for the peaks in the dynamic structure factor and for the propagating nature of the modes. The second component provides a means for satisfying the orthogonality and completeness conditions without imposing the Q^2 dependence of the modes density at a given frequency holding for plane waves. With respect to the Debye behavior, this could give rise to a pile-up of states at an energy to be identified with the boson peak energy.

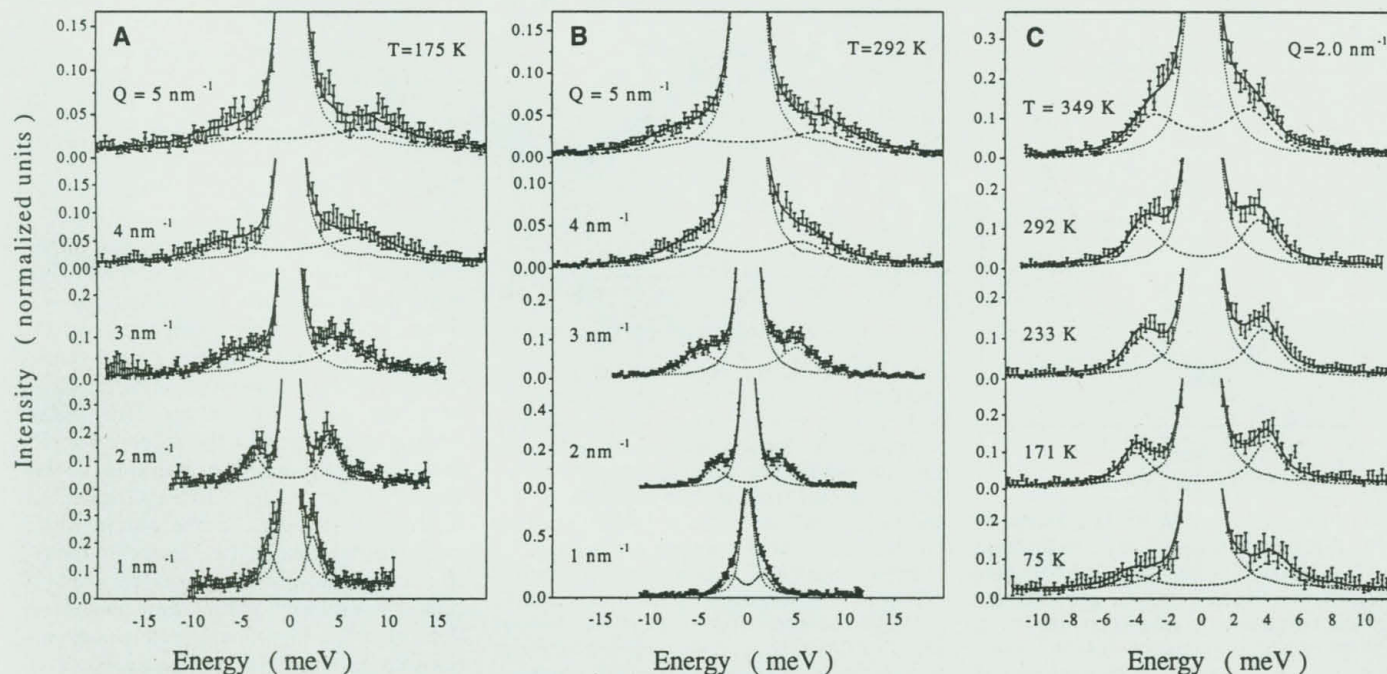


Fig. 3. (A) IXS spectra of glassy glycerol at 175 K at the indicated Q values. The data (\circ), shown with the error bars, are superimposed to the fit (solid line) as explained in the text. The dashed and dotted lines represent the quasi-elastic and inelastic contributions, respectively, to the total fits. The

data are normalized to the central peak intensity. The typical counting time was 100 s/point. (B) as in (A) for liquid glycerol at 290 K. (C) IXS spectra of glycerol at $Q = 2 \text{ nm}^{-1}$ at the indicated temperatures. Symbols and lines are as in (A).

Studies on the temperature dependence of the IXS spectra, such as those reported in Fig. 3C, provide insights into the evolution of the spectroscopic parameters, $\Omega(Q, T)$ and $\Gamma(Q, T)$, across the glass transition region (Fig. 5). At $Q = 2 \text{ nm}^{-1}$, the parameter $\Omega(Q, T)$ exhibits a clear temperature dependence with a slope-change in a temperature region not far from T_g , while the parameter $\Gamma(Q, T)$ has a smoother behavior within the statistical uncertainties (Fig. 5A). A quantitative analysis of these observations leads to the identification of two linear functions that represent the whole set of $\Omega(Q, T)$ data. They cross each other at a temperature indicated as $T_x = 300 \pm 20 \text{ K}$. This temperature marks the beginning of a much steeper reduction of the excitations energy in the liquid phase with increasing temperature; we suggested that, in the considered high-frequency limit, T_x marks the microscopic transition between two different dynamical regimes, characteristic of the glass and liquid phases (14). In view of the considered Q - E region, this transition can be interpreted as the freezing of the diffusional degrees of freedom at the

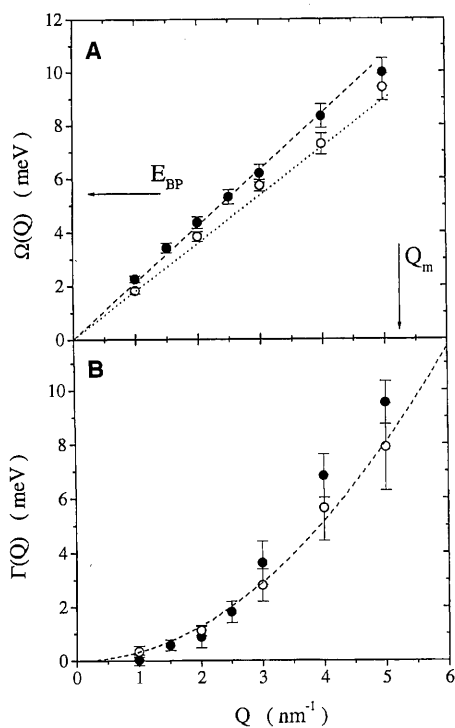


Fig. 4. Q -dependence of (A) the $\Omega(Q, T)$ and (B) the $\Gamma(Q, T)$ parameters, as derived from the fits at $T = 175 \text{ K}$ (●) and $T = 290 \text{ K}$ (○). The error bars correspond to $\pm 1\sigma$ statistical error, obtained from the fit as the parameter variation necessary to modify the best χ^2 value by one standard deviation, σ_{χ^2} . The lines, linear in (A) and quadratic in (B), are guides to the eye. The horizontal arrow indicates the boson peak energy in glycerol at T_g ; the vertical arrow indicates Q_m , defined by the relation $\Omega(Q_m) = \Gamma(Q_m)$.

molecular scale. These results demonstrate that even at high frequency, the dynamics are affected by the structural arrest taking place at the glass transition. In this respect, it is of great interest to compare the temperature evolution of the sound velocity measured at “high” and “low” Q values, because this quantity is very sensitive to structural relaxation processes. In particular, the IXS and BLS values of $v(Q)$ are expected to be the same in the low-temperature glass, because there are no relaxation processes at the time scales of the two probes. In contrast, in the liquid, the IXS values of the sound velocity, $v_{\text{IXS}}(Q)$, are expected to be larger than the BLS ones. This is because the BLS sound velocity has a steep temperature-dependent decrease due to the interference with the structural (α) relaxation. Comparison of experimental data for glycerol (Fig. 5B) shows that in the

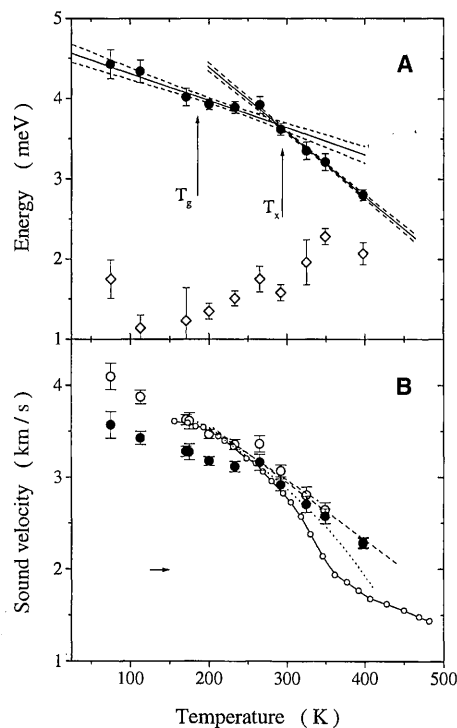


Fig. 5. (A) Temperature dependence of $\Omega(Q, T)$ (●) and $\Gamma(Q, T)$ (○) derived from the glycerol data at $Q = 2 \text{ nm}^{-1}$. The error bars correspond to $\pm 1\sigma$ statistical error. The solid lines are the best fits to the points in the low- and high-temperature regions, and they cross at $T_x = 300 \pm 20 \text{ K}$. The dashed lines indicate the limits of the $\pm 1\sigma$ prediction bands. The glass-transition temperature, T_g , is also indicated. (B) Temperature dependence of different sound velocities in glycerol: (●) $v_{\text{IXS}}(Q, T) = \Omega(Q)/Q$ obtained from (A); (○) $v_{\infty}(T)$ derived from the $Q \rightarrow 0$ limit of $v_{\text{IXS}}(Q, T)$ as described in the text; (—○—) $v(T)$ as derived from BLS measurements at $Q \approx 0.025 \text{ nm}^{-1}$; Dashed and dotted lines are the $v_{\infty}(T)$ values extrapolated in the liquid from low-temperature BLS data from (19) and (20), respectively.

glass, the value of $v_{\text{IXS}}(Q)$ at $Q = 2 \text{ nm}^{-1}$ is below the BLS data. This behavior is explained by the presence of a downward bending of the dispersion curve, leading to $v_{\text{IXS}}(Q) < v_{\text{IXS}}(0) = \lim_{Q \rightarrow 0} v_{\text{IXS}}(Q)$. This bending may have a structural origin, similar to what is observed in the acoustic phonon branches of crystals. The values of $v_{\text{IXS}}(0)$, obtained by considering a cubic term in the analysis of the dispersion curves, show satisfactory agreement with the BLS data in the glass region. Consequently, with the use of this correction, it is possible to identify $v_{\text{IXS}}(0)$ with the infinite frequency sound velocity, v_{∞} (23). This quantity, which represents the sound velocity at a frequency much larger than the inverse of the structural relaxation time, could not be experimentally determined before. Determination of its value is necessary to extract reliable values for τ from the BLS line-shapes (31) and to determine the nonergodicity factor $f_Q(T)$ (32). The values of v_{∞} have also been obtained from the IXS dispersion curves in other glass-formers such as *o*-terphenyl and *poly*-butadiene, with results confirming those in glycerol (14). From these latter studies, it has been possible to derive $f_Q(T)$ using two independent procedures, based either on the inelastic-to-elastic intensity ratio or on the value of v_{∞} itself. These preliminary results, although still affected by a large error bar, are consistent with the Model-Coupling Theory predictions. There are good reasons to believe that higher accuracy data are within reach in the near future, and consequently, it should be possible to perform stringent tests on different theoretical approaches to the liquid-glass transition.

Conclusions

The IXS technique allows the detailed study of the high-frequency dynamics of disordered systems. One of the most important results obtained so far is the finding that propagating collective excitations exist down to wavelengths comparable to the interparticle separation, and that they preserve an acoustic-like propagating character up to these high frequencies. This general finding, together with the specific temperature and exchanged momentum dependences of the spectral features, contributes to the understanding of the way in which microscopic dynamical processes are related to macroscopic phenomena in these materials. For example, it has been possible to show that the high-energy acoustic excitations could contribute to the excess of vibrational states and to the boson peak. Insights into the shape of the eigenvectors of these modes has been gained, and there is hope to relate this shape to the Q^2 -depen-



dence found for the $S(Q,E)$ broadening, $\Gamma(Q)$, which is still an open issue. Similarly, the experimental determination from the IXS data of the infinite frequency sound velocity allows investigation of the effect of structural relaxations in the high-frequency limit, aiding the analysis of BLS data, and possibly, the description of the liquid-glass transition by the derivation of the ergodicity factor.

The discussion in this paper has been limited to a special class of disordered systems, namely the glass-forming liquids exemplified here by glycerol. The IXS method is being applied, however, to other materials such as water and hydrogen-bonded liquids (8, 33), and neon and helium in supercritical conditions and at high density (34). Results obtained for these apparently very different systems can be interpreted within a framework very similar to that presented here, that is, relating the microscopic collective dynamics to phenomena such as particle collisions, diffusion, and structural relaxation processes in general.

REFERENCES AND NOTES

1. J. M. Ziman, *Models of Disorder* (Cambridge Univ. Press, Cambridge, 1979).
2. S. R. Elliot, *Physics of Amorphous Materials* (Longman, New York, 1990).
3. U. Balucani and M. Zoppi, *Dynamics of the Liquid State* (Clarendon Press, Oxford, 1994).
4. P. W. Anderson, B. I. Halperin, C. M. Varma, *Philos. Mag.* **25**, 1 (1972).
5. S. W. Lovesey, *Theory of Neutron Scattering from Condensed Matter* (Clarendon, Oxford, 1984).
6. U. Buchenau, H. M. Zhou, N. Nucker, K. S. Gilroy, W. A. Phillips, *Phys. Rev. Lett.* **60**, 1318 (1988).
7. J.-B. Suck, P. A. Egelstaff, R. A. Robinson, D. A. Sivia, A. D. Taylor, *Europhys. Lett.* **19**, 207 (1992); *J. Non-Cryst. Solids* **150**, 245 (1992); U. Buchenau, C. Pecharrroman, R. Zorn, B. Frick, *Phys. Rev. Lett.* **77**, 659 (1996).
8. F. Sette *et al.*, *Phys. Rev. Lett.* **75**, 850 (1995).
9. *European Synchrotron Radiation Facility Foundation Phase Report* (ESRF, Grenoble, France, 1987).
10. R. Verbeni *et al.*, *J. Synchrotron Radiat.* **3**, 62 (1996).
11. F. Sette, G. Ruocco, M. Krisch, C. Masciovecchio, R. Verbeni, *Phys. Scripta* **T66**, 48 (1996).
12. C. Masciovecchio *et al.*, *Nucl. Instrum. Methods Phys. Res. B* **111**, 181 (1996); *ibid.* **117**, 339 (1996).
13. W. Schulke, in *Handbook on Synchrotron Radiation*, G. Brown and D. E. Moncton, Eds. (Elsevier Science, Amsterdam, Netherlands, 1991), vol. 3, pp. 563–637.
14. C. Masciovecchio *et al.*, *Phys. Rev. B* **55**, 8049 (1997) [SiO_2]; G. Monaco, C. Masciovecchio, G. Ruocco, F. Sette, *Phys. Rev. Lett.* **80**, 2161 (1998) [*o*-terphenyl and *n*-butylbenzene]; A. Mermet *et al.*, *ibid.*, p. 4209 [*poly*-methyl-methacrylate]; L. Borjesson *et al.*, in preparation [CKN]; D. Fioretto *et al.*, in preparation [*poly*-butadiene].
15. P. Benassi *et al.*, *Phys. Rev. Lett.* **77**, 3835 (1996).
16. C. Masciovecchio *et al.*, *Phys. Rev. Lett.* **76**, 3356 (1996); C. Masciovecchio *et al.*, *ibid.* **80**, 544 (1998).
17. C. A. Angell, *J. Non-Cryst. Solids* **131**, 13 (1991).
18. M. Elwenspoek, M. Soltwisch, D. Quitmann, *Mol. Phys.* **34**, 33 (1977); *ibid.* **35**, 1221 (1978); J. Wuttke *et al.*, *Phys. Rev. Lett.* **72**, 3052 (1994); J. Wuttke, W. Petry, G. Coddens, F. Fujara, *Phys. Rev. E* **52**, 4026 (1995).
19. Y. X. Yan, L. T. Cheng, K. A. Nelson, *J. Chem. Phys.* **88**, 6477 (1988).
20. D. A. Pinnow, S. J. Candau, J. T. La Macchia, T. A. Litovitz, *J. Acoust. Soc. Am.* **43**, 131 (1968).
21. B. J. Berne and R. Pecora, *Dynamic Light Scattering* (Wiley-Interscience, New York, 1976).
22. B. Fak and B. Dörner, "On the Interpretation of Phonon Lineshapes and Excitation Entries in Neutron Scattering Experiments," Report No. 92FA008S (Institute Laue Langevin, Grenoble, France, 1992).
23. J. P. Boon and S. Yip, *Molecular Hydrodynamics* (Dover, New York, 1991).
24. G. Monaco, D. Fioretto, C. Masciovecchio, G. Ruocco, F. Sette, in preparation.
25. U. Buchenau *et al.*, *Phys. Rev. B* **34**, 5665 (1986).
26. A. P. Sokolov, U. Buchenau, W. Steffen, B. Frick, A. Wischniewski, *ibid.* **52**, R9815 (1995).
27. A. P. Sokolov, A. Kisliuk, D. Quitmann, E. Duval, *ibid.* **48**, 7692 (1993).
28. A. Brodin, A. Fontana, L. Borjesson, G. Carini, L. M. Torell, *Phys. Rev. Lett.* **73**, 2067 (1994).
29. See, for example, *Philos. Mag.* **B 71** (1995), *V International Workshop on Disordered Systems*, Andalo, 1994; *ibid.* **B 77** (1998), *VI International Workshop on Disordered Systems*, Andalo, Italy, 1997.
30. V. Mazzacurati, G. Ruocco, M. Sampoli, *Europhys. Lett.* **34**, 681 (1996).
31. M. Soltwisch, J. Sulmanowski, D. Quitmann, *J. Chem. Phys.* **86**, 3207 (1986); S. Loheider, G. Voegler, I. Petscherizin, M. Soltwisch, D. Quitmann, *ibid.* **93**, 5436 (1990); J. Tao, G. Li, H. Z. Cummins, *Phys. Rev. B* **43**, 5815 (1991); H. Z. Cummins, C. Dreyfus, W. Goetze, G. Li, R. M. Pick, *Phys. Rev. E* **50**, 4847 (1994); D. Fioretto, C. Palmieri, G. Socino, L. Verdini, *Phys. Rev. B* **50**, 605 (1994); M. Soltwisch *et al.*, *Phys. Rev. E* **57**, 720 (1998).
32. M. Fuchs, W. Götz, A. Latz, *Chem. Phys.* **149**, 185 (1990).
33. F. Sette *et al.*, *Phys. Rev. Lett.* **77**, 83 (1996); G. Ruocco *et al.*, *Nature* **379**, 521 (1996).
34. A. Cunsolo *et al.*, *Phys. Rev. Lett.* **80**, 3515 (1998).
35. We acknowledge A. Cunsolo, A. Mermet, M. Soltwisch, and R. Verbeni for their involvement in some of the IXS experiments reported here. We also thank U. Balucani, D. Fioretto, Y. Petroff, and M. Sampoli for useful discussions and their support to our work.

27 January 1998; accepted 23 April 1998

So instant, you don't need water...

NEW! SCIENCE Online's Content Alert Service

There's only one source for instant updates on breaking science news and research findings: SCIENCE's Content Alert Service. This free enhancement to your SCIENCE Online subscription delivers e-mail summaries of the latest research articles published each Friday in SCIENCE – **instantly**. To sign up for the Content Alert service, go to SCIENCE Online – and save the water for your coffee.

SCIENCE
www.sciencemag.org

For more information about Content Alerts go to www.sciencemag.org. Click on Subscription button, then click on Content Alert button.